by $q < -bNA/4\pi^2 C_B$ before stable regions of Z-structure occur. When q satisfies this condition, unique non-zero values of n and τ_Z exist which minimize the conformational free energy[5]. These are

$$n = -qA - (bNA^2/4\pi^2 C_B) \quad (3)$$

$$\tau_B = \tau_Z = -bA/2\pi C_B \quad (4)$$

where $0 < n < N_Z$. (If the segment is sufficiently underwound that $n = N_Z$, then $\tau_z = \tau_B$ is found from equation (1). To illustrate these results we use values $C_B = 8.5 \times 10^{-12}$ erg base pair rad^{-2} and $b = 0.8$ kcal mol^{-1} from the literature[4,7]. Then a segment must be underwound by 0.33 deg per base pair before the onset of transition to structures containing stable Z-form regions. When deformed beyond this threshold, enough susceptible base pairs switch to Z-structure for the twist rates to be maintained at $\tau_B = \tau_Z = -0.33$ deg per base pair. Only when the segment is so underwound that all susceptible sequences are in the Z-form do τ_B and τ_Z decrease below -0.33 deg per base pair.

To augment the above treatment we apply the statistical mechanical theory of two state transitions in torsionally stressed DNA[6] to the present problem. This renders computable the transition probability profiles of specific base sequences, which more accurately reflect the fluctuational character of these transitions.

The partition function for this transition is[6]

$$Z = \sum_{n=0}^{N_Z} \left[I_n \sum_{r_n} (s^n \sigma^\gamma) \right] \quad (5)$$

where r_n enumerates all states containing n Z-form base pairs, s is the equilibrium constant for a susceptible base pair, σ is the cooperativity factor and γ is the number of beginnings of sequences of base pairs in the Z-form. Also,

$$I_0 = \exp(-2\pi^2 q^2 C_B \beta/N), \quad (6a)$$

$$I_n = \left(\frac{2\pi(N-n)}{NnC_B\beta}\right)^{1/2} \exp\left(\frac{-2\pi^2 C_B \beta (q + n/A)^2}{N}\right), \quad 0 < n \leq N_Z \quad (6b)$$

From this partition function one can determine transition profiles, the expected value of τ_B and other equilibrium properties of the system as described in ref. 6. Figure 1 shows the results of a sample calculation carried out on a sequence of 80 base pairs, of which 8 were susceptible to the transition. Note that because the enthalpy of the B–Z transformation is zero[4], this two-state transition is not thermal in character, but rather depends primarily on the imposed torsional deformation q.

We have presented two theoretical analyses of transitions between B-form and Z-form in torsionally stressed DNA. In this initial formulation the possible role of local denaturation (perhaps necessary at the junction between B-form and Z-form regions, for example) has not been considered. A three-state treatment of this problem will be presented elsewhere. Despite lack of precise knowledge of several important parameters (torsional stiffness C_Z, cooperativity factor σ), the present analysis predicts that B–Z transitions could occur in response to the torsional deformations consequent on (negative) DNA superhelicity. In principle, it is possible that similar transitions also occur between other conformational states of the DNA. It has been suggested that stress-induced conformational transitions at defined sequences may serve diverse regulatory functions by altering the accessibility of the bases[5].

Received 25 February; accepted 19 May 1980.

1. Wang, A. *et al. Nature* **282,** 680–686 (1979).
2. Wang, J. *Proc. natn. Acad. Sci. U.S.A.* **76,** 200–204 (1979).
3. Levitt, M. *Proc. natn. Acad. Sci. U.S.A.* **75,** 640–644 (1978).
4. Pohl, F. & Jovin, T. *J. molec. Biol.* **67,** 375–396 (1972).
5. Benham, C. *Proc. natn. Acad. Sci. U.S.A.* **76,** 3870–3874 (1979).
6. Benham, C. *J. chem. Phys.* **72,** 3633–3639 (1980).
7. Barkley, M. & Zimm, B. *J. chem. Phys.* **70,** 2991–3007 (1979).
8. Crick, F., Wang, J. & Bauer, W. *J. molec. Biol.* **129,** 449–461 (1979).

0028–0836/80/320638—03$01.00

Metarhodopsin I/metarhodopsin II transition triggers light-induced change in calcium binding at rod disk membranes

U. B. Kaupp, P. P. M. Schnetkamp & W. Junge

Universität Osnabrück, Schwerpunkt Biophysik, Postfach 4469, D-4500 Osnabrück, FRG

The hypothesis of Yoshikami and Hagins[1] that calcium ions act as diffusible transmitter molecules between the photochemistry of rhodopsin and the subsequent electrical events at the outer plasma membrane of rods initiated many investigations on light-stimulated calcium release in vertebrate photoreceptor cells (see refs 2, 3). Although it now seems firmly established that light has some effect on the redistribution of calcium in various disk preparations[2,4,5], reconstituted systems[6,7] and intact rod outer segments[3,8], the physiological significance remained unclear. We previously reported a rapid, light-triggered calcium release from binding sites at the disk membrane in the presence of calcium ionophore A23187 (refs 3, 8). However, there is no evidence for rapid calcium release into the cytosol in the absence of ionophore. On fragmentation of intact rod outer segments, calcium release due to a light-regulated change of calcium binding appeared almost completely abolished[3,8]. We describe here experiments with sonicated rod outer segments in which the previously observed loss of the calcium release capacity has been prevented. Calcium release in sonicated disks in the presence of A23187 kinetically follows the metarhodopsin I/metarhodopsin II transition ($\tau_{1/2} = 10$ ms, activation energy $E_A = 34$ kcal mol^{-1}), suggesting that calcium release is triggered by this photochemical transition.

Intact cattle rod outer segments have been isolated according to Schnetkamp *et al.*[9]. Disk vesicles were obtained by sonication of intact rod outer segments in a medium containing sucrose, 600 mM; Ficoll 400, 5% v/v; HEPES, *p*H 7.0 2 mM, for 30 s at 40 W. The suspension also contained about 3–4 μM of free calcium introduced by the stock suspension of rod outer segments.

Inhibition of calcium release can be prevented by keeping the ionic strength of the final suspension medium below 5 mM of 1:1 electrolyte, irrespective of the fragmentation procedure (lysis or sonication) and the fragmentation conditions (for example, high or low ionic strength). We conclude that the apparent abolition of the release capacity in fragmented rods is caused by regulation of calcium binding by cations other than calcium which had no access to the site of calcium release in both rods with a leaky and an intact plasma membrane.

Rapid calcium release was followed by means of kinetic flash spectrophotometry with the calcium indicator arsenazo (III). Details on working with arsenazo (III) and the principle and instrumentation of flash spectrophotometry have been reviewed elsewhere[3,10]. In a suspension of sonicated disks buffered with only 2 mM HEPES at *p*H 6.8, *p*H measurements with the *p*H indicators bromcresol purple and Mg-arsenazo (III) (ref. 11) demonstrated that the total proton buffering capacity (membranes and HEPES) is sufficient to suppress light-induced *p*H changes which might give rise to *p*H-induced absorption changes of arsenazo (III) (not shown). To obtain kinetically undistorted recordings of calcium release in sonicated material at higher time resolution (Fig. 1*a*), signals due to the intrinsic photochemistry of arsenazo (III) (ref. 3) have been recorded separately and subtracted from the superimposed calcium-indicating signals by means of a signal averager with a data reduction program (Nicolet 1072). The signal-to-noise ratio was improved by sampling of signals over several repetitions from one cuvette.

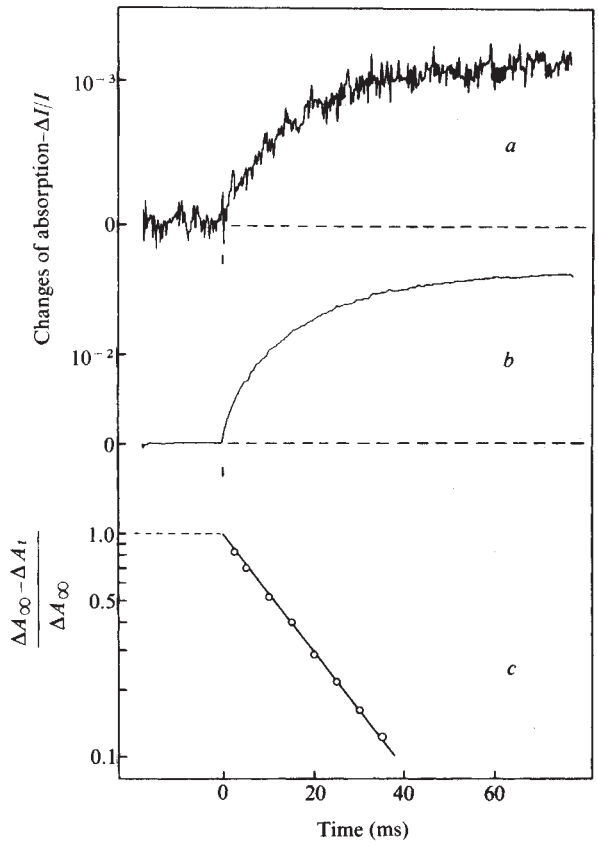

Fig. 1 Time course of the light-induced absorption changes at: *a*, 655 nm and *b*, 382 nm after excitation of sonicated rod outer segments by a flash at $t = 0$ in the presence of arsenazo (III) and A23187. Signals were obtained by averaging from one sample over 16 repetitions for *a* and four repetitions for *b* at a frequency of 0.5 Hz. The optical bandwidth of the measuring beam was 16 nm, the electrical integration time 200 μs. Further conditions as in Fig. 2. *c*, Semilogarithmic plot of the calcium-indicating absorption change from part *a*.

The half-rise time of flash-induced calcium release in the presence of equal amounts of A23187 (10 μM) depends on the structural integrity of rod outer segments (Fig. 2). In intact rod outer segments, calcium release occurs more slowly ($\tau_{1/2}$ = 300 ms) than in sonicated disk vesicles ($\tau_{1/2}$ = 10 ms). Unlike its kinetics, the stoichiometry of calcium released/rhodopsin bleached is comparable in both preparations (~0.4 calcium/rhodopsin*). Light-triggered calcium release in sonicated material is depicted in Fig. 1*a* at a higher time resolution. A semilogarithmic plot of the absorption changes from Fig. 1*a* reveals that the time course of calcium release can be described by a single first order reaction (Fig. 1*c*). Concomitantly in intact rod outer segments and sonicated suspensions the metarhodopsin I/metarhodopsin II transition has been recorded at 382 nm. A half-rise time of about 10 ms at 20 °C and at *p*H 7 was observed for both preparations. The time course of this photochemical transition is shown for sonicated disk vesicles in Fig. 1*b*. From inspection of Fig. 1 it is evident that the time course of rapid calcium release in sonicated rods in these conditions closely parallels that of the metarhodopsin I/metarhodopsin II transition.

To determine the energy of activation for both processes, the temperature dependence of the respective rate constants has been investigated in similar conditions (Fig. 3). Rate constants have been calculated from overall half-rise times according to $1/\tau_{1/2} = k(\ln 2)^{-1}$. The metarhodopsin I/metarhodopsin II transition exhibits *p*H- and temperature-dependent biphasic kinetic behaviour (ref. 12 and our unpublished observation) and therefore two ways of analysing the data have been adopted. First, the overall rate constants of the metarhodopsin I/metarhodopsin II transition are shown in Fig. 3 (closed circles). They match reasonably well with the calcium release data (triangles). If only the rate constant of the slower kinetic component is considered (Fig. 3, open circles) the correspondence, especially for higher temperatures, is even better. This is due to the temperature dependence of the relative amplitudes of the two kinetic phases of the metarhodopsin I/metarhodopsin II transition which favours the rapid component at higher temperatures[12]. Notwithstanding this subtlety of a biphasic kinetic behaviour of the metarhodopsin I/metarhodopsin II transition, it is obvious from Fig. 3 that both reactions have a similar activation energy of about 34 kcal mol^{-1}.

The similarity of activation energies and time constants of both reactions strongly suggests that the calcium release system is intimately coupled to the metarhodopsin I/metarhodopsin II transition. In agreement with this notion is the linear relationship between metarhodopsin II formation and the amount of calcium release reported earlier[3,8].

The rapid rise time of the calcium-indicating absorption changes in sonicated vesicles probably reflects the actual time required for the trigger step to occur. The diffusion time of calcium ions from binding sites through the suspending medium to an indicator molecule[13] as well as the relaxation time of complex formation between arsenazo (III) and calcium[14] are too short to contribute significantly to the time course of the calcium-monitoring absorption changes. The mechanism underlying the slower kinetics in intact rod outer segments probably involves an additional reaction step and will be considered elsewhere[15], but from the present study it is obvious that in the presence of 10 μM A23187 the kinetics of calcium release are not rate limited by the ionophore.

For the actual release step two distinct mechanisms may be considered. In the first model, calcium is bound directly to rhodopsin and released during the metarhodopsin I/metarhodopsin II transition due to a change of the electrostatic interaction between calcium and its coordination groups at the rhodopsin molecule. This change could involve spatial separation of chelating groups accompanying conformational changes

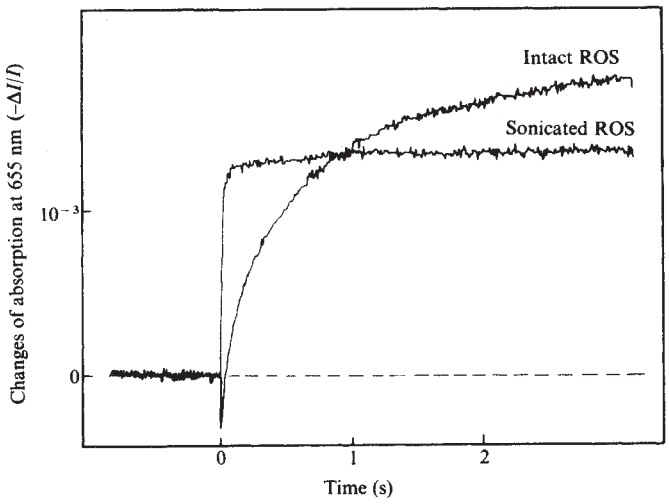

Fig. 2 Time course of the light-induced absorption changes at 655 nm after excitation of intact and sonicated rod outer segments (ROS) by a flash at $t = 0$ in the presence of arsenazo (III) and ionophore A23187. Suspension medium contained: sucrose, 600 mM; HEPES, 2 mM; Tris, 0·5 mM at *p*H 7.0; arsenazo (III), 30 μM; A23187, 10 μM; free calcium concentration 3–4 μM and rhodopsin, 3.5 μM. Fraction of rhodopsin bleached/flash about 4%. Cuvette path length 10 mm. Temperature, 20 °C. Excitation wavelength, 530 nm; half duration of excitation flash 10 ns. Signals were obtained by averaging from one sample over four repetitions at a frequency of 0.1 Hz.

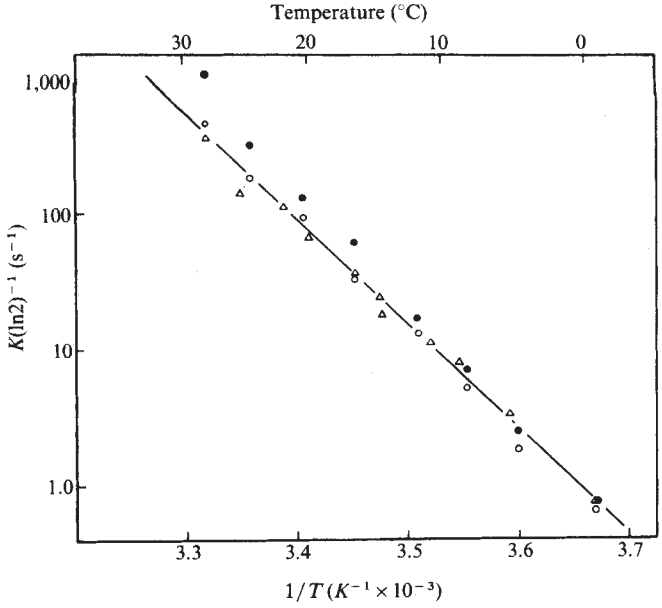

Fig. 3 Arrhenius plot of the temperature dependence of the calcium release (△), the metarhodopsin I/metarhodopsin II transition (●), and the slow component of the metarhodopsin I/metarhodopsin II transition (○) in sonicated rod outer segments. Further conditions as in Fig. 2.

within rhodopsin. In the second model, a reorientation of molecular dipoles within the rhodopsin molecule or rapid proton uptake[16] could decrease an interfacial potential at the disk membrane. According to $K_D = K_D^0 \exp(-2e\varphi/kT)$ the apparent binding constant K_D of calcium binding sites (not necessarily on rhodopsin) is dependent on the surface potential φ (K_D^0 = binding constant in the absence of any interfacial potential). Consequently any change of an interfacial potential will result in a redistribution of calcium bound to the membrane.

It is difficult to decide between the models outlined above. The close correlation between calcium release and the metarhodopsin I/metarhodospin II transition could be interpreted in favour of the first model. However, the fact that rapid calcium release is completely abolished when rod outer segments are dissolved in either nonylglucose (gift of Dr W. J. de Grip, Nijmegen) or Triton X-100 (not shown) would be difficult to explain if calcium were directly bound to rhodopsin. A more detailed account of the interrelationship between calcium release, rapid proton uptake and interfacial potentials will be published elsewhere[15].

This work was financially supported by the Deutsche Forschungsgemeinschaft.

Received 21 February; accepted 19 May 1980.

1. Yoshikami, S. & Hagins, W. A. *Biophys. J. Abstr.* **16,** 35a (1971).
2. Smith, H. G., Fager, R. S. & Litman, B. J. *Biochemistry* **16,** 1399–1405 (1977).
3. Kaupp, U. B., Schnetkamp, P. P. M. & Junge, W. in *Detection and Measurement of Free Ca^{2+} in Cells* (eds Ashley, C. C. & Campbell, A. K.) 287–308 (Elsevier, Amsterdam, 1979).
4. Shevchenko, T. F. *Biophysics* **21,** 327–330 (1976).
5. Smith, H. G., Jr. & Bauer, P. J. *Biochemistry* **18,** 5067–5073 (1979).
6. O'Brien, D., Zumbulyadis, N., Miachaels, F. M. & Ott, R. A. *Proc. natn. Acad. Sci. U.S.A.* **74,** 5222–5226 (1977).
7. Hubbell, W. L., Fung, K.-K., Hong, K. & Chen, Y. S. in *Vertebrate Photoreception* (eds Barlow, H. B. & Fatt, P.) 41–59 (Academic, London, 1977).
8. Kaupp, U. B., Schnetkamp, P. P. M. & Junge, W. *Biochim. biophys. Acta* **552,** 390–403 (1979).
9. Schnetkamp, P. P. M., Klompmakers, A. A. & Daemen, F. J. M. *Biochim. biophys. Acta* **552,** 379–389 (1979).
10. Junge, W. in *Chemistry and Biochemistry of Plant Pigments* Vol. II (ed. Goodwin, T. W.) 233–333 (Academic, London, 1976).
11. Russell, J. T. & Martonosi, A. N. *Biochim. biophys. Acta* **544,** 413–429 (1978).
12. Hoffman, W., Siebert, F., Hofmann, K. P. & Kreutz, W. *Biochim. biophys. Acta* **503,** 450–461 (1978).
13. Kaupp, U. B. thesis, Univ. Berlin (1979).
14. Scarpa, A., Brinley, F. J. Jr. & Dubyak, G. *Biochemistry* **17,** 1378–1386 (1978).
15. Kaupp, U. B., Schnetkamp, P. P. M. & Junge, W. (in preparation).
16. Emrich, H. M. *Z. Naturforsch.* **B26,** 352–356 (1971).

A novel conformation of valinomycin in its barium complex

S. Devarajan, C. M. K. Nair, K. R. K. Easwaran & M. Vijayan

Molecular Biophysics Unit, Indian Institute of Science, Bangalore–560 012, India

Knowledge of the molecular mechanisms involved in ionophore-mediated cation transport would be valuable for understanding many essential functions of biological membranes[1–3]. Cations are transported in several stages, such as formation of the ionophore–cation complex, diffusion across the cell membrane and subsequent release of the cation. Several conformational rearrangements are involved in this process, and so a detailed understanding of all the conformational possibilities of the ionophore seems to be essential for elucidating the molecular mechanism of ion transport. We are carrying out spectroscopic and crystallographic studies to explore the possible conformational stages of ionophores by complexing them, in different solvents, with cations of various sizes and charges. We report here a novel conformation of the ionophore valinomycin in its barium complex. It can be described as an extended depsipeptide chain, without internal hydrogen bonds, wound in the form of an ellipse with the two barium ions located at the foci.

Spectroscopic studies in solution (for example, circular dichroism (CD) spectra shown in Fig. 1) carried out by us indicated that the conformation of valinomycin in its barium complex was different from those in uncomplexed valinomycin and its complex with monovalent cations. Barium perchlorate and barium thiocyanate were used to investigate complexation

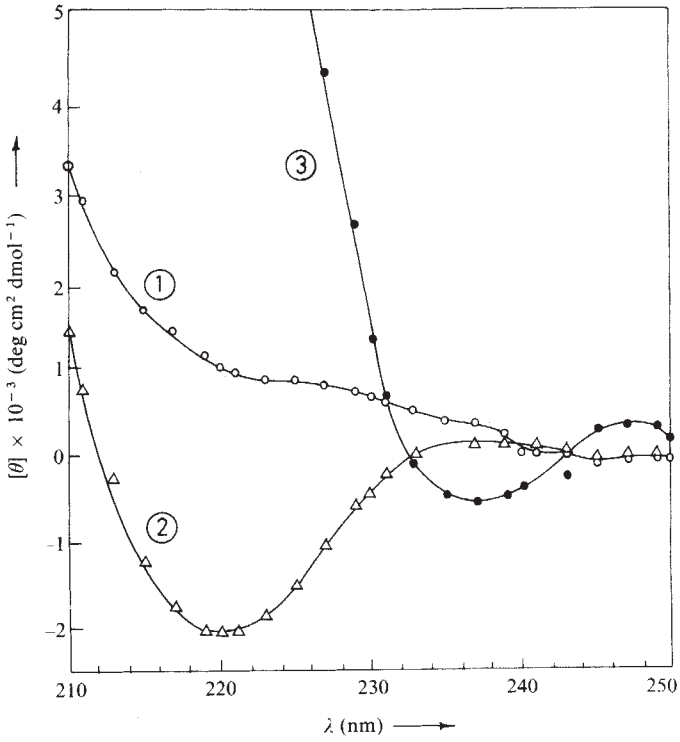

Fig. 1 CD spectra in acetonitrile of free valinomycin (○), its 1:2 barium perchlorate complex (△) and its 1:1 potassium perchlorate complex (●). The concentration of valinomycin was 29 mM (○, △) and 9 mM (●). In the potassium perchlorate complex the molar ellipticity, $[\theta]$, continuously increases with decrease in λ with a $[\theta]$ value of 25,000 deg cm^2 per dmol at λ = 210 nm.

0028–0836/80/320640—02$01.00